Microfluidic origami: a new device format for in-line reaction monitoring by nanoelectrospray ionization mass spectrometry†

Andrea E. Kirby[a] and Aaron R. Wheeler*[ab]

Microfluidics is an attractive platform for chemical synthesis because it offers fast reaction times, reduced reagent usage, and the ability to integrate multiple functions on a single device. Digital Microfluidics (DMF) is particularly well-suited for microscale chemical synthesis, as it permits discretized sample handling, allowing for total process control. However, a limitation of DMF-based synthesis is analysis, which is often performed offline. To this end, we have developed ''microfluidic origami'', a new device format that integrates DMF with in-line analysis by mass spectrometry (MS). This format comprises a DMF platform and a folded nanoelectrospray ionization (nanoESI) emitter formed on a single flexible polyimide film substrate. Additionally, the device contains a two-plate-to-one-plate DMF interface, which allows for straightforward coupling of micro-reaction operations and product delivery to the emitter for analysis. The integrated platform was used to perform the Morita–Baylis–Hillman (MBH) reaction using DMF followed by inline MS analysis for monitoring the reaction progress in real-time. We propose that this platform has potential as a new tool for real-time monitoring of reaction rates and reaction pathways and could be a useful addition to the synthetic organic chemistry laboratory.

Introduction

Microfluidic chemical synthesis is popular because it offers reduced reagent consumption and processing times, rapid heat exchange, and the capacity to integrate multiple functions on a single device.[1,2] The standard format for microfluidics, planar devices bearing enclosed microchannels, is particularly well-suited to miniaturized flow chemistry, which allows for fast reactions, access to short-lived intermediates, and the potential for scale-up to form large amounts of products.[3–5] An alternative format for miniaturized fluid-handling, digital microfluidics (DMF), uses electric fields to manipulate individual microdroplets on insulated electrode arrays.[6] Digital microfluidics can be operated in a one-plate format[7–9] (in which droplets are positioned on top of a single substrate bearing electrodes) or a two-plate format[10,11] (in which droplets are sandwiched between two substrates), and is growing in popularity as a complementary approach to methods relying on microchannels.

The discretized nature of sample handling in DMF makes it uniquely useful for micro-batch chemical synthesis. Millman *et al.*[12] were the first to use DMF for applications related to synthesis, forming patterned microparticles on a one-plate DMF device; progress was monitored visually by microscopy. Dubois *et al.*[13] used DMF in the one-plate format to perform Grieco's reaction, a three component reaction that produces a tetrahydroquinoline. The reaction products were analyzed offline by chromatography and mass spectrometry (MS), and in-line using cyclic voltammetry directly on the DMF device. Jebrail *et al.*[14,15] used two-plate DMF to synthesize peptide macrocycles and peptidomimetic products, which were evaluated offline using MS and NMR. A two-plate DMF method for chemical synthesis of 2-[¹⁸F]fluoro-2-deoxy-D-glucose (a common tracer for PET imaging) was developed by van Dam and coworkers[16,17] and quality control of the product was assessed off-device. These examples highlight the great advantage of using DMF for chemical synthesis: individual manipulation of multiple reagents on a single device permits complete control over multi-step reactions.

A challenge for DMF- based chemical synthesis is detection. As is evident from the examples above, this is often accomplished offline, whereby reaction product droplets are taken off the device for analysis using a benchtop instrument. In the case of mass spectrometry, this typically means evaporating, resolubilizing and pipetting from the device, and dilution in a MS-appropriate solvent before analysis.[18,19]

[a]*Department of Chemistry, University of Toronto, 80 St George St., Toronto, ON, M5S 3H6, Canada. E-mail: aaron.wheeler@utoronto.ca; Fax: +1 (416) 946 3865; Tel: +1 (416) 946 3864*
[b]*Institute of Biomaterials and Biomedical Engineering, 164 College Street, Toronto, ON, M5S 3G9, Canada*
† Electronic supplementary information (ESI) available. See DOI: 10.1039/c3lc41431k

This process is undesirable, as it adds time and introduces additional handling steps. There have been only three inline interfaces for DMF and MS reported in the literature, all coupling droplet processing with electrospray ionization (ESI) MS. The first is a device containing both a DMF module and a microchannel nanoESI emitter.[20] A challenge for this system is the labour-intensive fabrication steps required to make the devices. A second technique uses an eductor interface, comprising a transfer capillary inserted between the plates of a two-plate DMF device connected to a tapered gas nozzle and a metal ESI emitter.[21] Droplets are pulled from the DMF device to the emitter by a pressure differential generated when a pulse of gas is applied to the nozzle. The third inline interface for DMF and ESI MS[22] consists of a pulled glass capillary nanoESI emitter inserted between the top and bottom substrates of the two-plate DMF device. Although the latter two examples are relatively simple to setup and operate, they both require external hardware and alignment of the emitter with respect to the DMF device, which can be tricky.

Here we report the first DMF system used for microchemical synthesis coupled to mass spectrometry. This innovation builds on the work of (1) Abdelgawad et al.,[23] who reported one-plate DMF devices made from flexible substrates that can be used to move droplets on non-planar surfaces (in a phenomenon known as "All-Terrain Droplet Actuation," or ATDA), and (2) Kirby et al.,[24] who developed folded nanoESI emitters made from a similar flexible substrate. Here, we have combined these techniques to form an integrated device format that we call "microfluidic origami," comprising a DMF device and nanoESI emitter on a single flexible substrate. Moreover, we report a new two-plate-to-one-plate DMF interface (relying on conventional definitions of these formats), which allows for transfer of droplets between a dispensing and mixing region and an analysis region of a device. Finally, we have used this device for in-line monitoring of the Morita–Baylis–Hillman (MBH) reaction. We speculate microfluidic origami will eventually be useful for real-time analysis of reaction rates and reaction pathways for a wide range of microscale synthetic processes.

Experimental

Reagents and materials

Polyimide tape (87.5 μm total thickness; 50 μm polyimide with 37.5 μm silicone adhesive) was purchased from Argon Masking, Inc. (Monrovia, CA, USA). Unless otherwise specified, reagents were obtained from Sigma Aldrich (Oakville, ON, Canada). Photolithography reagents were from Rohm and Haas (Marlborough, MA, USA) and CR-4 chromium etchant was from Cyantek (Fremont, CA, USA). Parylene-C dimer was purchased from Specialty Coating Systems (Indianapolis, IN, USA) and Teflon-AF was from Dupont (Wilmington, DE, USA). HPLC grade methanol and deionized water (diH$_2$O) with a resistivity of 18 MΩ cm at 25 °C were used in all experiments. MBH reagent and catalyst solutions were prepared in diH$_2$O from pure standards at the following concentrations: 100 mM

2-pyridine carboxaldehyde, 130 mM methyl acrylate, and 65 mM 2,2-diazobicyclooctane (DABCO).

DMF-nanoESI device fabrication and assembly

Polyimide tape substrates were adhered to glass slides and coated with metal (20 nm chromium adhesion layer and 100 nm gold) and AZ1500 photoresist by Telic (Valencia, CA, USA). These substrates were used to form DMF device bottom plates in the University of Toronto Emerging Communications Technology Institute (ECTI) cleanroom facility using conventional techniques. Briefly, the substrates were UV exposed (365 nm, 29.8 mW cm^{-2}, 10 s) through a transparent photomask (Pacific Arts and Design, Markham, ON, Canada) using a Karl-Süss MA6 mask aligner (Garching, Germany). They were then developed in MF321 (3 min) and post-baked on a hot plate (100 °C, 2 min) before being immersed in gold etchant (30 s) and then CR-4 (1 min). The remaining photoresist was removed in AZ300T (10 min), and the substrates were rinsed with acetone and methanol, dried under a stream of nitrogen, and dried on a hot plate (90 °C, 2 min). Patterned contact pads and the tip of the MS spray voltage wire (see below) were covered in low-tack dicing tape (Semiconductor Equipment Corporation, Moorpark, CA, USA) before coating with 2.2 μm of Parylene-C using a vapour deposition instrument (Specialty Coating Systems, Indianapolis, IN, USA). 200 nm of Teflon-AF was applied by spin coating (1% wt/wt solution in Fluorinert FC-40, 1600 rpm, 60 s) followed by post-baking on a hot plate (160 °C, 10 min).

DMF device top plates were prepared from indium tin oxide (ITO) coated polyethylene terephthalate (PET) (60 Ω sq^{-1}, 125 μm thickness) from Sigma Aldrich (Oakville, ON, Canada). Each substrate (approximately 32 × 50 mm) was adhered to a glass microscope slide using high strength acrylic adhesive (300LSE, 3M, London, ON, Canada). The glass slide was shorter than the ITO PET film substrate such that there was a 10 mm overhang of film at one edge. These substrates were also coated with Teflon AF (200 nm, as above), and the bare edge of the ITO PET film was coated with Teflon-AF by wiping with a lint-free swab that had been dipped in 1% wt/wt Teflon-AF in FC-40 before a post-bake on a hot plate (160 °C, 10 min).

As shown in Fig. 1(a), the DMF device comprises three distinct regions: the two-plate DMF platform, the one-plate DMF platform and the folded nanoESI emitter. The two-plate DMF region includes 19 square actuation electrodes (2.2 × 2.2 mm each), four reagent reservoir electrodes (three 5 × 5 mm and one 4.75 × 6.68 mm), one mixing electrode (4.75 × 6.68 mm, with a single 2.2 × 2.2 mm electrode cutout) and a trapezoidal electrode (bases 6.68 mm and 2.8 mm, length 6.68 mm), with inter-electrode gaps of 40–130 μm. The one-plate DMF region includes a linear array of 12 square electrodes (2.8 × 2.8 mm each) separated by 40 μm inter-electrode gaps, a DMF counter electrode ground wire (1 mm wide) separated from the square electrodes by a 40 μm gap, and a MS spray voltage wire (250 μm wide) that is separated from the DMF counter-electrode by a 200 μm gap. Both wires are adjacent to the linear array of square electrodes across the length of the one-plate region of the device. Each driving and ground electrode on the bottom plate is connected to a series of contact pads (not shown).
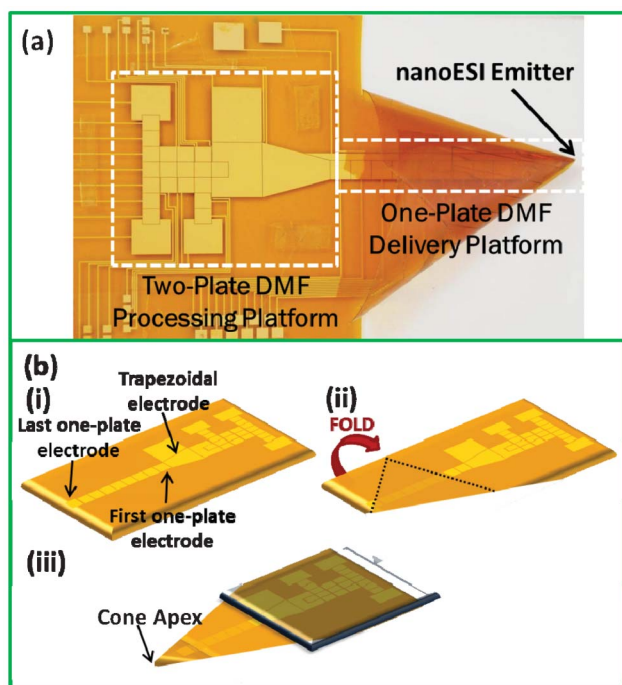
Fig. 1 Microfluidic origami. (a) Photo of the device highlighting three distinct regions: the two-plate DMF processing platform to perform microscale chemical processes, the one-plate DMF delivery platform to actuate processed droplets to the emitter, and the folded polyimide nanoESI emitter. (b) Schematic depicting the device assembly process. The polyimide substrate is cut at the edge of the last one-plate electrode (i), the one-plate region of the device is folded into the conical nanoESI emitter with the last one-plate electrode at the cone apex (ii), and the top plate is positioned on the two-plate region of the device (iii).

Each device was assembled in three steps. First, the bottom substrate was trimmed with a scalpel at the edge of the last electrode on the one-plate region (Fig. 1(b)(i)). Second, the dicing tape was removed (exposing the contact pads and the MS spray voltage wire), and the edge of the device was manually folded into a cone (Fig. 1(b)(ii)) with a ~50 μm orifice such that the apex of the cone was positioned at the edge of the last one-plate electrode. Third, the top plate (ITO-PET mounted on glass) was positioned above the two-plate DMF region of the bottom plate and joined by spacers formed from three pieces of double-sided tape (total spacer thickness 210 μm) as in Fig. 1(b)(iii). Care was taken to position the edge of the ITO-PET film (overhanging the glass support, as described above) above the trapezoidal electrode patterned on the bottom substrate, such that the edge of the top-plate overlapped the first square electrode of the one-plate DMF portion of the device by ~200–300 μm.

DMF device operation

Driving potentials were generated by amplifying the sine wave output of a function generator (Agilent Technologies, Santa Clara, CA, USA) operating at 18 kHz. Reagent and solvent droplets were initially pipetted onto reagent reservoirs and sandwiched between the top and bottom plates of the two-plate region of the device, and were actuated by applying driving potentials (210–260 V_{rms}) between the top-plate

electrode (ground) and sequential electrodes on the bottom substrate *via* the exposed contact pads. To actuate a droplet from the two-plate to one-plate regions of the device, the top-plate electrode and the counter electrode wire on the bottom plate were both grounded and the driving potential was increased to 380–420 V_{rms} as the droplet traversed the interface. A video depicting this process (and the reverse, with a droplet moving from the one-plate to the two-plate region) can be found in the online supporting information. Once the droplet was on the one-plate region, the driving potential was maintained at 380–420 V_{rms} and was applied between the grounded counter electrode wire and the adjacent driving electrodes.

DMF-driven chemical synthesis

A six-step method was developed to implement the MBH reaction with in-line analysis by mass spectrometry. First, 7 μL aliquots of the two reagents and the catalyst were loaded into the designated reagent reservoirs and 15 μL of diH$_2$O was loaded into the water reservoir. Second, 1.1 μL droplets of each reagent and the catalyst (three droplets in total) were actively dispensed[10,11] from the large reservoir droplets onto the array of driving electrodes, and the three reagent droplets were merged and incubated for 1, 5 or 10 min. For the 5 and 10 min incubation times, the reaction droplet was actively mixed[25] for 1 min and left stationary for the remaining incubation time, while the 1 min actuation time was not actively mixed. Third, the reaction droplet was driven to the large mixing electrode and merged with the 15 μL diH$_2$O droplet. Fourth, the diluted droplet was actuated from the two-plate region to the one-plate region of the device (as above). Fifth, an 18 μL droplet of MeOH containing 0.1% formic acid (FA) was pipetted onto the fifth electrode on the one-plate region. Sixth, the product droplet was merged with the acidified MeOH droplet to form a final ~36 μL solution for analysis.

Inline MS analysis

The device was placed on an *xyz*-positioning stage (Parker Automation, Cleveland, OH, USA) ~3 mm from the grounded inlet of an LTQ linear ion trap mass spectrometer (Thermo Scientific, Waltham, MA, USA). A processed reaction droplet was actuated along the one-plate portion of the device to the apex of the folded nanoESI emitter; a video depicting this process can be found in the online supporting information. The DMF driving potential and ground connections were then disconnected from the device, and the spray voltage was applied to the solution *via* the dedicated wire patterned adjacent to the DMF electrodes. The transfer capillary temperature was 200 °C for all experiments. Applied potentials were varied in the range of +2–3 kV for each experiment performed with a unique device to optimize the observed signal. The spectra were obtained by averaging 5 acquisitions (at a rate of 6 acquisitions/s). Images of the electrospray were collected using a CCD camera positioned perpendicular to emitters ~3 mm from the grounded inlet of the mass spectrometer.

Results and discussion

The overall goal of this work was to develop an integrated microfluidic platform for chemical synthesis with in-line analysis by mass spectrometry for reaction monitoring. Towards this goal, three innovations were required: a two-plate to one-plate DMF interface, a DMF-active nanoelectrospray ion source for mass spectrometry, and a DMF microreactor. Together, these innovations (which are described below) constitute "microfluidic origami," a new format for in-line analysis of microreactions.

Two-plate to one-plate DMF interface

There are two distinct formats of digital microfluidics: two-plate DMF, in which droplets are confined between a bottom substrate bearing patterned working electrodes and a conductive top substrate counter electrode, and one-plate DMF, where droplets are free-standing on a single substrate patterned with both the working and grounded counter electrodes. The two-plate format is advantageous in that it is compatible with all droplet movement operations (dispensing from reservoirs, merging, mixing, and splitting), and thus useful for performing processes in a controlled manner. The two-plate format was necessary for the goals of this project, as it allowed for sequential dispensing of reagents for multistep organic synthetic reactions. In contrast, the one-plate DMF format is not compatible with droplet dispensing from reservoirs, limiting its utility to simple processes that do not require complex droplet manipulation. However, the one-plate format was particularly attractive for this work because Abdelgawad et al.[23] demonstrated that it can be implemented on flexible, non-planar substrates; we hypothesized that similar methods might be compatible with folded nanoelectrospray emitters for mass spectrometry.[24] Unfortunately, in the vast majority of cases, digital microfluidic devices are formed for one-plate or two-plate operation, not for both. Thus, our goals dictated the development of a new device format, comprising one-plate and two-plate regions integrated on a single device.

To our knowledge, there has been only one previous report[26] of a device incorporating both two-plate and one-plate regions. This creative format[26] is unique, relying on a ground wire (a "catena") suspended above the bottom plate. Most DMF devices do not use suspended wires, which can be tricky to assemble and prepare, and are likely not compatible with folded nanoESI emitters. Moreover, the authors of the report[26] acknowledge that the interface between the two-plate and one-plate regions of the device is not perfect; droplets translating between the two regions often become pinched or stuck. Therefore for our new method, we strove to develop a reliable interface for translating droplets between two-plate and one-plate regions on a device not requiring suspended wires for operation.

After some trial and error, we developed the format depicted in Fig. 2(a). In this format, the top plate serves as the ground electrode for droplets in the two-plate region of the device, and a wire patterned adjacent to the working electrodes on the bottom-plate serves as the ground electrode on the one-plate region of the device. As shown, droplets can be translated from the two-plate region to the one-plate region and back again (a corresponding video can be found in the online supplementary information). After optimization, droplet translation across the interface was observed to be facile and smooth, and in quantitative studies, in 78 trials on 50 devices, 94% of
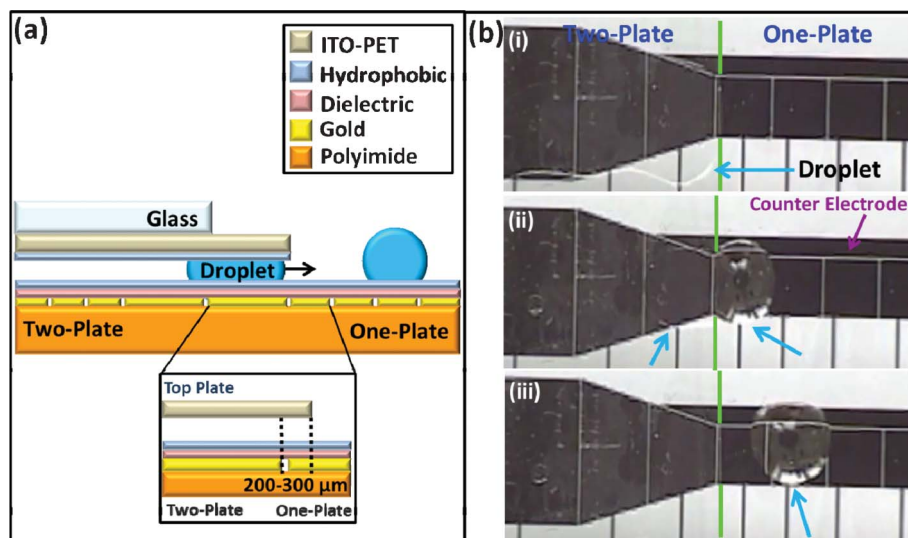

Fig. 2 Two-plate to one-plate interface for microfluidic origami. (a) Side-view schematic of the interface. The two-plate region of the device contains the bottom polyimide film substrate with patterned gold electrodes, and the top grounded counter electrode made of ITO-coated PET film. A portion of the top substrate contains glass backing to provide stability. The one-plate region of the device contains a single substrate patterned with both the working and ground electrodes. (b) Frames from a movie depicting droplet motion across the interface; the green lines show the boundary between the two-plate (left side) and one-plate (right side) regions of the device. In frame (i), the droplet (blue arrow) is in the two-plate region of the device; in frame (ii), the droplet is straddling the interface; in frame (iii), the droplet is in the one-plate region of the device.

the droplets moved through the interface without becoming stuck.

In developing the optimized device format shown in Fig. 2, we observed three design elements that were required for reliable droplet translation through the interface. The first is related to the thickness of the material used for the device top-plate. In initial trials using a conventional top-plate formed from a 1 mm thick ITO-coated glass microscope slide, droplets were observed to become stuck at the interface, a consequence of touching the thick hydrophilic edge of the top plate. In contrast, when we used a 125 μm-thick top plate formed from ITO-coated PET film, droplets moved smoothly through the interface without sticking to the top substrate. The second design element concerns the placement of the top-plate in relation to the interface. In initial studies, we found that placing the edge of the top-plate directly at the junction between the final two-plate electrode and the first one-plate electrode lead to droplet pinching at the interface. Likewise, placing the edge of the top-plate ~500 μm or more over-lapping the first one-plate electrode also resulted in droplet pinching. On balance, we found that positioning the edge of the top-plate such that it overlaps the first electrode on the one-plate region by ~200–300 μm, as depicted in Fig. 2(a), combined with simultaneous grounding of both the top-plate counter-electrode and the one-plate patterned ground wire, prevented droplet pinching and improved droplet movement fidelity. The third design element is related to the shape and size of the working electrodes at the interface. As can be seen in Fig. 1(b), the actuation electrodes on the two-plate portion of the device close to the interface have a larger footprint (6.8 mm × 6.8 mm) than the electrodes further from the interface (2.8 mm × 2.8 mm). This allows for comparable droplet volumes to be accommodated on both regions of the device. The final electrode on the two-plate region at the interface is trapezoidal in shape; it tapers from the width of the two-plate electrodes to the smaller width of the one-plate electrodes. This tapering was found to help prevent droplet pinching at the sides of the electrodes as droplets traverse the interface, allowing for smooth droplet movement. We acknowledge that more work is needed to characterize the fluid mechanics of this type of interface (this was not the focus of this work); we propose that the three design elements described here are a good starting point for future study.

Finally, we note that the new two-plate to one-plate DMF interface was optimized for aqueous droplet transportation. In preliminary studies, we have observed that the interface works well for aqueous-organic solvent mixtures that contain less than 15% methanol or acetonitrile, but that droplets with higher ratios of organic content cannot traverse the interface, even with increased actuation voltages. We hypothesize this is related to surface tension, as droplets of lower surface tension are more favoured to remain suspended between the top and bottom substrates of a two-plate DMF device than droplets of higher surface tension liquids. We propose that future studies may be able to overcome this limitation (if needed) *via* a comprehensive evaluation of droplet, device, and electrode geometry.

Integrated nanoESI emitter

There is growing interest in the development of inexpensive and accessible alternatives[27–30] to the commonly used pulled glass capillary nanoESI emitters for sample introduction for mass spectrometry. For example, folded emitters[24] were recently reported as a low-cost alternative, and are quickly and easily formed by bending a flexible film into a cone shape with a micron-sized orifice at the apex (Fig. 3(a)). Folded emitter performance has been validated for diverse analytes across a wide mass range, with performance similar to that of pulled-glass capillary emitters. We hypothesized that folded emitters would be compatible with All-Terrain Droplet Actuation (ATDA),[24] in which microfluidic samples are manipulated on non-planar single-plate digital microfluidic devices. Here we describe this combination, which represents the first report of DMF coupled to ESI MS in a completely integrated fashion, whereby the DMF device and nanoESI emitter are formed from a single substrate.

As shown in Fig. 3(b), devices were formed by patterning a linear array of square actuation electrodes adjacent to (1) a counter-electrode for DMF actuation, and (2) a patterned wire for applying the ESI spray voltage. The substrate was then folded to form a nanoESI tip such that the orifice aligned with the end of the electrode array. As shown in Fig. 3(c), droplets could be transported along the array into the confined geometry of the emitter tip (a corresponding video can be
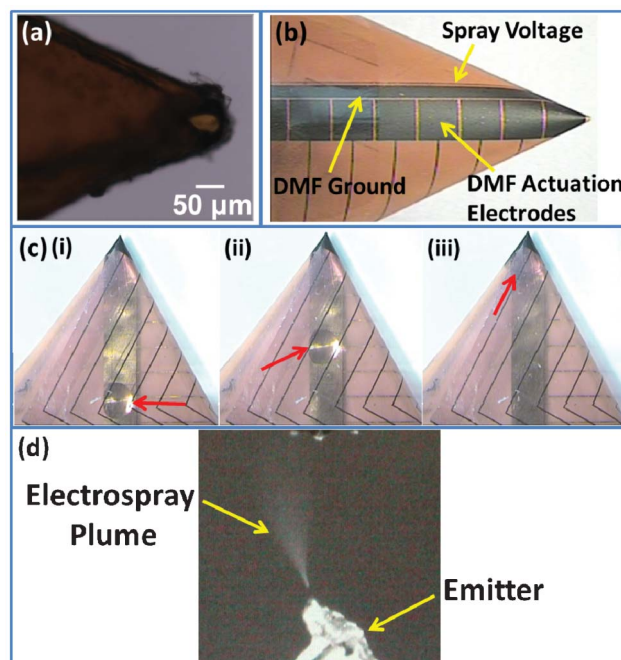

Fig. 3 Microfluidic origami nanoESI MS emitter. (a) Picture of the apex of a folded polyimide nanoESI emitter. (b) Picture of the folded nanoESI emitter portion of a microfluidic origami device. A thin wire patterned adjacent to the DMF working and counter electrodes acts as the electrical connection for the spray voltage. (c) Frames from a movie depicting a droplet (red arrows) being actuated on the one-plate DMF portion of the device into the nanoESI emitter. (d) Picture of a Taylor cone generated when a high DC potential is applied to a droplet in the folded emitter.

found in the online supplementary information). Droplets readily moved into the cone and made contact with the bottom, top, and sides of the substrate. In fact, in 105 trials on 20 devices, droplets were successfully delivered to the cone in 100% of the cases.

After delivery of a sample droplet to the emitter apex by DMF actuation, the spray voltage was applied to the patterned wire to form the Taylor cone, as shown in Fig. 3(d). The tip of this wire is free of the dielectric and hydrophobic coatings to ensure full contact with the sample. In initial trials, we observed that wires of widths of 500 μm and greater were susceptible to corona discharge. Using a thinner wire prevented this; thus, in the final design, a 250 μm thick wire was used, which allowed for full contact of the spray voltage with the sample droplet with no discharge.

Microchemical synthesis with in-line reaction monitoring

The Morita–Baylis–Hillman (MBH) reaction was selected to validate the utility of the microfluidic origami device format. The MBH reaction involves reaction of an aldehyde with an α,β-unsaturated electron withdrawing group catalyzed by DABCO to produce an allylic alcohol. The reaction scheme is shown in Fig. 4(a); the aldehyde used is 2-pyridinecarboxaldehyde, and the α,β-unsaturated ketone is methyl acrylate. The MBH reaction was a good match for this work for a number of reasons. First, this reaction is easily monitored *in situ*, and the catalytic cycle has been extensively characterized by ESI-MS.[31–33] The starting materials, reaction intermediates, and product all have easily discernible $[M + H]^+$ peaks in the mass spectrum,

which can be seen in catalytic cycle in Fig. 4(b). Second, the reaction is particularly straightforward to perform on a DMF device: it simply involves mixing of reagents, no heating or cooling is required, the reaction proceeds rapidly under ambient conditions, and the reaction intermediates and product all remain in solution. A third advantage of the MBH reaction for this application is that it can be performed in aqueous conditions, and the reaction rate is accelerated in water over organic solvents.[34] This is particularly useful given the limitations on solvent transport across the two-plate to one-plate interface (see above).

The steps involved in performing the MBH reaction on-device are shown in Fig. 4(c). The reservoirs on the two-plate portion of the device are loaded with the reagents and the catalyst, equivolume droplets of each are dispensed onto the working electrode array and merged, and the reaction mixture incubates (Fig. 4(c)(i–iii)). After the incubation period, the reaction droplet is actuated to the central large square electrode and merged with a water droplet to dilute the reaction mixture (Fig. 4(c)(iv)). The droplet is then translated across the two-plate to one-plate interface as in Fig. 2(b), and merged with an acidified methanol droplet. This step quenches the reaction, dilutes the products, and forms a solvent suitable for nanoESI MS. The droplet is then translated along the one-plate portion of the device to the apex of the folded nanoESI emitter as in Fig. 3(c). The DMF actuation voltage is disconnected and the spray voltage is connected, making contact with the solution in the emitter tip *via* the
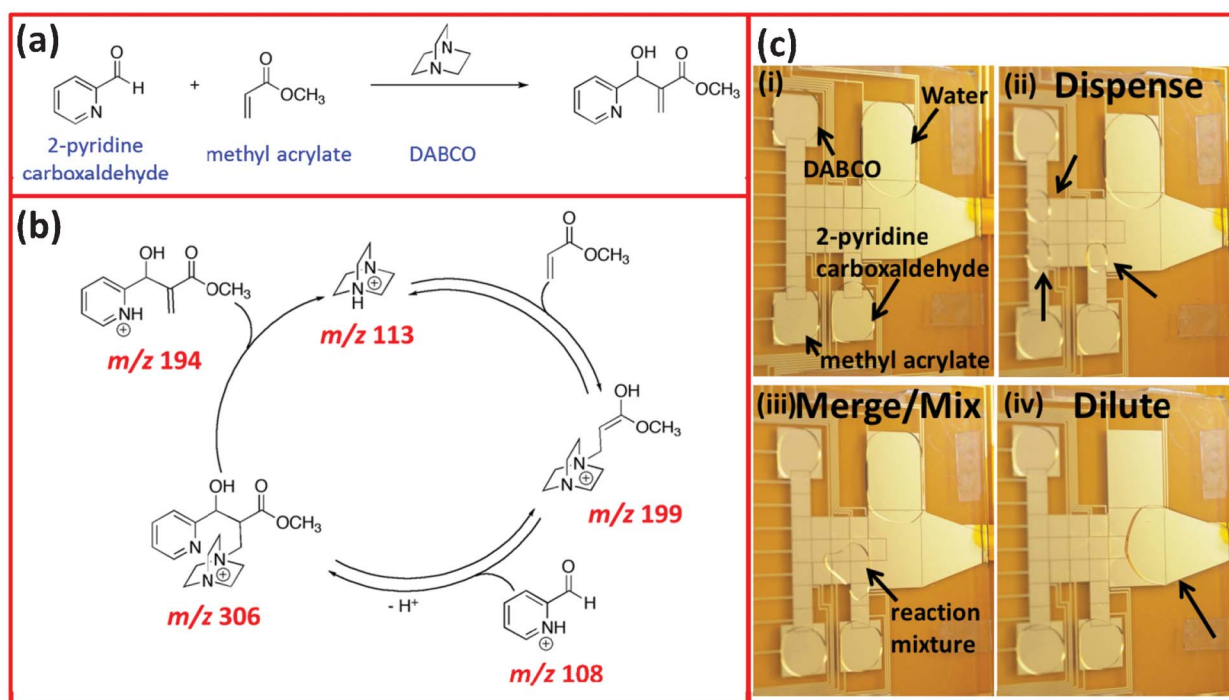

Fig. 4 MBH microreaction enabled by microfluidic origami. (a) MBH reaction scheme of 2-pyridinecarboxaldehyde with methyl acrylate in the presence of DABCO to yield an allylic alcohol product. (b) The catalytic cycle of the MBH reaction showing all reaction species that can be seen in the mass spectrum, and their associated *m/z*. (c) Frames from a movie depicting the steps involved in performing the MBH reaction on-device. Equivolume droplets of each reagent are dispensed, merged, mixed, and allowed to react for a specified time, followed by dilution in water.

patterned spray voltage wire on the device. A spray is generated (as in Fig. 3(d)) and mass spectra are collected.

Performance of the integrated DMF-nanoESI MS platform for the MBH reaction was evaluated by collecting mass spectra at three reaction time points. A full mass spectrum can be seen in Fig. 5(a). Peaks corresponding to five components of the MBH catalytic cycle are present: starting materials 2-pyridine carboxaldehyde at m/z 108 and DABCO at m/z 113, intermediate 1 at m/z 199, intermediate 2 at m/z 306, and the product at m/z 194. Sub-spectra generated at three different reaction times for three components of the catalytic cycle (intermediate 1, intermediate 2, and product) are shown in Fig. 5(b). Each set of spectra for individual components are expressed on the same absolute intensity scale, but the absolute intensity scales for each set of spectra are different. The [M + H] peak at m/z 199 for intermediate 1 increases significantly in intensity over the reaction times monitored, from 7.5×10^5 counts at 1 min to 7.3×10^6 counts at 10 min reaction time. Likewise, the [M + H] peak intensity for intermediate 2 at m/z 306 increases from 1.5×10^5 counts at 1 min to 1.6×10^6 counts at 10 min reaction time. Similar results are found for the product [M + H] peak at m/z 194; at 1 min reaction time the peak has an intensity of 5.6×10^4 counts, which increases to 5.1×10^5 counts at 10 min reaction time. These results suggest that reaction progress can be seen after only 10 min of reaction time, and monitoring peak intensity over longer incubation times could provide insight into the reaction rate and reaction completion time.

The results shown in Fig. 5 validate the microfluidic origami method for implementing chemical microreactions with in-line analysis by mass spectrometry. In ongoing work, we are developing means to (a) dispense sub-samples of products for analysis at multiple time points from a single device (in contrast to the proof-of-principle methods described here in which the entire product droplet was consumed in each analysis) and (b) use suitable internal standards for absolute quantitation of intermediates and products. Given the growing interest in the use of digital microfluidics for micro-synthesis,[12–17] we propose that the microfluidic origami method introduced here will be of interest to the lab-on-a-chip community, particularly for scientists without access to facilities capable of multi-layer microfabrication.

Conclusion

We have developed "microfluidic origami," a new digital microfluidic device format that enables in-line analysis of microchemical reactions. Microfluidic origami allows for integration of a DMF device and folded nanoESI emitter on a single flexible substrate, and also incorporates a functional two-plate-to-one-plate interface for DMF, which permits droplet transfer between a dispensing and mixing region and an analysis region on the same device. We used this device to qualitatively monitor the reaction progress of the Morita–Baylis–Hillman reaction in real time, which represents the first application of an in-line interface for DMF and MS with application to monitoring chemical synthesis. We propose that this new platform could find utility in synthetic organic chemistry for in-line monitoring of reaction rates and reaction pathways for a wide range of chemical reactions, as well as for investigating new reaction conditions on the microscale.
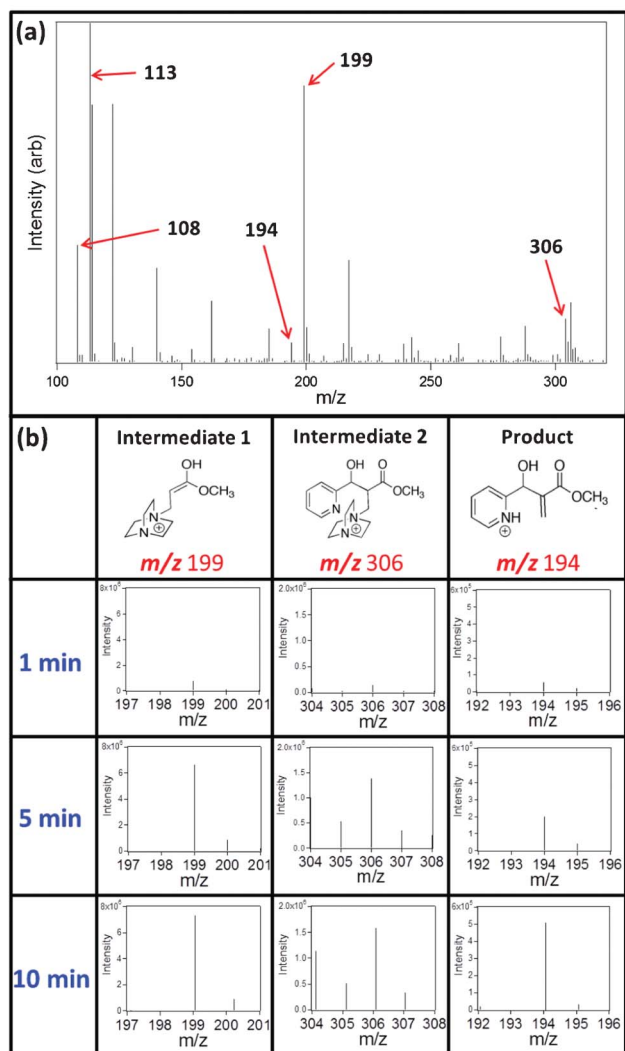

Fig. 5 Microfluidic origami for in-line reaction monitoring. (a) Mass spectrum of an MBH reaction implemented and analyzed on a microfluidic origami device. Labeled peaks include: 2-pyridine carboxaldehyde (m/z 108), DABCO catalyst (m/z 113), intermediate 1 (m/z 199), intermediate 2 (m/z 306), and reaction product (m/z 194). (b) Table of sub-spectra showing the changes in peak intensities of the reaction intermediates and product at three different time intervals. All spectra corresponding to each species are plotted with the same absolute intensity scale, but spectra for each species have different intensity scales.

Acknowledgements

References

1 K. Jähnisch, V. Hessel, H. Löwe and M. Baerns, *Angew. Chem., Int. Ed.*, 2004, **43**(4), 406–446.

2 A. J. de Mello, *Nature*, 2006, **442**(7101), 394–402.

3 C. Wiles and P. Watts, *Eur. J. Org. Chem.*, 2008, **2008**(10), 1655–1671.

4 X. Y. Mak, P. Laurino and P. H. Seeberger, *Beilstein J. Org. Chem.*, 2009, **5**, 19.

5 C. F. Carter, H. Lange, S. V. Ley, I. R. Baxendale, B. Wittkamp, J. G. Goode and N. L. Gaunt, *Org. Process Res. Dev.*, 2010, **14**(2), 393–404.

6 K. Choi, A. H. C. Ng, R. Fobel and A. R. Wheeler, *Annu. Rev. Anal. Chem.*, 2012, **5**(1), 413–440.

7 C. G. Cooney, C.-Y. Chen, M. R. Emerling, A. Nadim and J. D. Sterling, *Microfluid. Nanofluid.*, 2006, **2**, 435–446.

8 U.-C. Yi and C.-J. Kim, *J. Micromech. Microeng.*, 2006, **16**, 2053–2059.

9 M. Abdelgawad and A. R. Wheeler, *Adv. Mater.*, 2007, **19**, 133–137.

10 M. G. Pollack, R. B. Fair and A. D. Shenderov, *Appl. Phys. Lett.*, 2000, **77**, 1725–1726.

11 S. K. Cho, H. Moon and C.-J. Kim, *J. Microelectromech. Syst.*, 2003, **12**, 70–80.

12 J. R. Millman, K. H. Bhatt, B. J. Prevo and O. D. Velev, *Nat. Mater.*, 2004, **4**, 98–102.

13 P. Dubois, G. Marchand, Y. Fouillet, J. Berthier, T. Douki, F. Hassine, S. Gmouh and M. Vaultier, *Anal. Chem.*, 2006, **78**, 4909–4917.

14 M. J. Jebrail, A. H. C. Ng, V. Rai, R. Hili, A. K. Yudin and A. R. Wheeler, *Angew. Chem., Int. Ed.*, 2010, **49**, 8625–8629.

15 M. J. Jebrail, N. Assem, J. M. Mudrik, M. D. M. Dryden, K. Lin, A. K. Yudin and A. R. Wheeler, *J. Flow Chem.*, 2012, **2**(3), 103–107.

16 P. Y. Keng, S. Chen, H. Ding, S. Sadeghi, G. J. Shah, A. Dooraghi, M. E. Phelps, N. Satyamurthy, A. F. Chatziioannu, C.-J. Kim and R. M. van Dam, *Proc. Natl. Acad. Sci. U. S. A.*, 2012, **109**(3), 690–695.

17 H. Ding, S. Sadeghi, G. J. Shah, S. Chen, P. Y. Keng, C.-J. Kim and M. van Dam, *Lab Chip*, 2012, **12**, 3331–3340.

18 V. N. Luk and A. R. Wheeler, *Anal. Chem.*, 2009, **81**, 4524–4530.

19 N. A. Mousa, M. J. Jebrail, H. Yang, M. Abdegawad, P. Metalnikov, J. Chen, A. R. Wheeler and R. F. Casper, *Sci. Transl. Med.*, 2009, **1**, 1ra2.

20 M. J. Jebrail, H. Yang, J. M. Mudrik, N. M. Lafreniere, C. McRoberts, O. Y. Al-Dirbashi, L. Fisher, P. Chakraborty and A. R. Wheeler, *Lab Chip*, 2011, **11**, 3218–3224.

21 C. A. Baker and M.G. Roper, *Anal. Chem.*, 2012, **84**, 2955–2960.

22 S. C. C. Shih, H. Yang, M. J. Jebrail, R. Fobel, N. McIntosh, O. Y. Al-Dirbashi, P. Chakraborty and A. R. Wheeler, *Anal. Chem.*, 2012, **84**, 3731–3738.

23 M. Abdelgawad, S. L. S. Freire, H. Yang and A. R. Wheeler, *Lab Chip*, 2008, **8**, 672–677.

24 A. E. Kirby, M. J. Jebrail, H. Yang and A. R. Wheeler, *Rapid Commun. Mass Spectrom.*, 2010, **24**, 3425–3431.

25 P. Paik, V. K. Pamula, M. G. Pollack and R. B. Fair, *Lab Chip*, 2003, **3**, 28–33.

26 J. Berthier, Ph. Clementz, J.-M. Roux, Y. Fouillet and C. Peponnet, *Modeling microdrop motion between covered and open regions of EWOD microsystems*, in NSTI Nanotechnology Conference and Trade Show-Nanotech, NSTI: Boston, USA, 2006, pp. 685–688.

27 S. Ksoyonov and P. Williams, *Rapid Commun. Mass Spectrom.*, 2001, **15**, 1890.

28 P. Liuni, T. Rob and D. J. Wilson, *Rapid Commun. Mass Spectrom.*, 2010, **24**, 315.

29 H. L. J. Wang, R. G. Cooks and Z. Ouyang, *Angew. Chem., Int. Ed.*, 2010, **49**, 877.

30 J. Liu, H. Wang, N. E. Manicke, J.-M. Lin, R. G. Cooks and Z. Ouyang, *Anal. Chem.*, 2010, **82**(6), 2463.

31 L. Silva Santos, C. Henrique Pavam, W. P. Almeida, F. Coelho and M. N. Eberlin, *Angew. Chem., Int. Ed.*, 2004, **43**, 4330–4333.

32 G. W. Amarante, H. M. S. Milagre, B. G. Vaz, B. R. Vilacha Ferreira, M. N. Eberlin and F. Coelho, *J. Org. Chem.*, 2009, **74**, 3031–3037.

33 V. G. Santos, T. Regiani, F. F. G. Dias, W. Romao, J. L. Paz Jara, C. F. Klitzke, F. Coelho and M. N. Eberlin, *Anal. Chem.*, 2011, **83**, 1375–1380.

34 J. Auge, N. Lubin and A. Lubineau, *Tetrahedron Lett.*, 1994, **35**(43), 7947–7948.